Int. J. Heat Mass Transfer. Vol. 20, pp. 953–960. Pergamon Press 1977. Printed in Great Britain

NATURAL CONVECTION EFFECTS ON GRAETZ PROBLEM IN HORIZONTAL ISOTHERMAL TUBES

JENN-WUU OU and K. C. CHENG
Department of Mechanical Engineering, University of Alberta, Edmonton, Alberta, Canada

(*Received* 30 *August* 1976 *and in revised form* 8 *December* 1976)

Abstract—The classical Graetz problem with natural convection effect in isothermally cooled or heated horizontal tubes is approached by a numerical method using large Prandtl number assumption. Numerical solutions are obtained for a range of Rayleigh numbers $Ra = 0$–10^6. The developing secondary flow and temperature fields, bulk temperature, local and average Nusselt numbers are presented to study the natural convection effect. The Nusselt number results are compared against the experimental data and the agreement is found to be satisfactory.

NOMENCLATURE

a, tube radius;
Gr, Grashof number, $g\beta(T_0 - T_w)a^3/\nu^2$;
g, gravitational acceleration;
h, average heat-transfer coefficient;
k, thermal conductivity;
Nu, local Nusselt number, $h(2a)/k$;
$\overline{Nu}$, average Nusselt number based on arithmetic mean temperature difference;
P, pressure deviation due to secondary flow;
Pr, Prandtl number, ν/κ;
p, $P/[Gr(\rho\nu^2)/a^2]$;
R, ϕ, Z, cylindrical coordinates;
Ra, Rayleigh number, $PrGr = g\beta(T_0 - T_w)a^3/\nu\kappa$;
Re, Reynolds number, $(2a)\overline{W}_f/\nu$;
r, z, z_0, R/a, $(Z/2a)/RePr$, and onset point (z) of free convection effect (see Fig. 9), respectively;
T, T_0, T_w, local temperature, uniform entrance temperature and constant wall temperature, respectively;
U, V, W_f, velocity components in R, ϕ directions and fully developed axial velocity, respectively;
u, v, $(U, V)/(\kappa/a)$;
$\overline{W}_f$, average axial velocity;
w_f, $W_f/\overline{W}_f = 2(1-r^2)$;
$\nabla^2_{r,\phi}$, $\partial^2/\partial r^2 + (1/r)\partial/\partial r + (1/r^2)\partial^2/\partial\phi^2$.

Greek symbols

β, coefficient of thermal expansion;
θ, θ_b, dimensionless temperature difference, $(T - T_w)/(T_0 - T_w)$, dimensionless bulk temperature, $(2/\pi)\int_0^{\pi}\int_0^1 w_f\theta r\,dr\,d\phi$;
κ, thermal diffusivity;
ν, kinematic viscosity;
ξ, vorticity, $\nabla^2_{r,\phi}\psi$;
ρ, density;
ψ, dimensionless stream function.

1. INTRODUCTION

THE CLASSICAL Graetz problem [1] for laminar forced convection in fully developed laminar flow through a tube with uniform wall temperature neglects the effect of buoyancy forces. When fluids are heated or cooled in forced flow through horizontal tubes or ducts, the resulting temperature differences give rise to density variations. Thus, the buoyancy forces always exist and one must assess the natural convection effects in practical applications [2].

For the case of horizontal tubes with constant wall temperature, the natural convection effect is important only in the thermal entrance region since the effect disappears as the bulk temperature approaches the wall temperature in the fully developed region. The experimental investigations on combined free and forced laminar convection in horizontal, isothermal tubes are well reviewed and summarized by Depew and August [3]. They give the empirical equation for average Nusselt number which correlates the published experimental data to within $\pm 40\%$. This suggests immediately the difficulty of the problem and the need for understanding the heat transport mechanism.

Recently, Hieber and Sreenivasan [4] carried out a theoretical analysis for mixed convection in an isothermally heated horizontal pipe with a uniform axial velocity profile at the pipe inlet for a large Prandtl number fluid. The analysis sheds considerable light on heat-transfer mechanism and represents a marked improvement over the existing empirical correlations [4]. At present, numerical analysis on combined free and forced laminar convection in the thermal entrance region of horizontal tubes or channels is possible only by using the large Prandtl number assumption [5–7]. The analysis using the Navier–Stokes and energy equations does not seem to have been extended to the technically important case of an isothermally cooled or heated horizontal tube. The analysis based on field equations provides a complete secondary flow and temperature fields for flow visualization. This is in contrast to the approximate analysis of Hieber and Sreenivasan [4] where one must assume five different

flow regimes in the thermal entrance region. Physically, one may distinguish clearly the Leveque solution region with negligible natural convection effect, the intermediate region and the fully developed region with again negligible natural convection effect. The physical nature of the problem is such that further subdivisions of the entrance region may not be so clear-cut and particularly the distinction may not be possible for low to intermediate Rayleigh number regime. In any case, a simpler and direct approach is highly desirable in view of the complexity of the problem.

The purpose of this paper is to present theoretical results of numerical analysis for Graetz problem with natural convection effect in horizontal, isothermal tubes using large Prandtl number assumption and Boussinesq approximation. With the present physical model, the main flow retains Poiseuille profile and the secondary flow is important only in the energy equation. The numerical results are compared with the available experimental data for Prandtl number of order one or greater.

The present problem is important in many industrial applications requiring the prediction of short-tube heat-transfer performance. One notes that the natural convection effect is also important in liquid solidification inside the cooled horizontal tubes with forced laminar flow [8, 9]. The liquid–solid interface represents the isothermal condition and the results of the present analysis may be used in assessing the importance of the natural convection effect on ice formation in horizontal circular tubes.

2. ANALYSIS

The formulation of the problem is discussed elsewhere [5, 7].

The governing equations in cylindrical coordinates [see Fig. 1(a)] using the dimensionless variables and parameters defined in Nomenclature can be shown to be

$$\nabla^2_{r,\phi}\xi = -Ra\left(\frac{\partial\theta}{\partial r}\sin\phi + \frac{1}{r}\frac{\partial\theta}{\partial\phi}\cos\phi\right) \tag{1}$$

$$\nabla^2_{r,\phi}\psi = \xi \tag{2}$$

$$\frac{1}{r}\frac{\partial}{\partial r}(ru\theta) + \frac{1}{r}\frac{\partial}{\partial\phi}(v\theta) + \frac{w_f}{4}\frac{\partial\theta}{\partial z} = \nabla^2_{r,\phi}\theta \tag{3}$$

where $w_f = 2(1-r^2)$ and $u = (1/r)\partial\psi/\partial\phi$, $v = -\partial\psi/\partial r$.

The boundary conditions are

$$\begin{aligned} &\theta = 1 \text{ at } z = 0 \text{ (uniform entrance temperature)}\\ &\theta = 0 \text{ at } r = 1 \text{ (uniform wall temperature)}\\ &\psi = \partial\psi/\partial r = 0 \text{ at } r = 1,\ \psi = \xi = \partial\theta/\partial\phi = 0\\ &\qquad\qquad \text{along } \phi = 0,\ \pi \text{ (symmetry).} \end{aligned} \tag{4}$$

It is noted that the inertia terms in the vorticity transport equation is neglected because of large Prandtl number assumption. The governing equations are seen to be elliptic in both vorticity and stream function, and parabolic in temperature.

The local Nusselt number, $Nu = h(2a)/k$, based on local wall temperature gradient and axial temperature gradient, respectively, can be written as

$$Nu_1 = -(2/\pi\theta_b)\int_0^{\pi}(\partial\theta/\partial r)_{r=1}\,d\phi \tag{5}$$

$$Nu_2 = -(1/2\pi\theta_b)\int_0^{\pi}\int_0^{1}(\partial\theta/\partial z)w_f\,r\,dr\,d\phi.$$

In experimental investigations, the average Nusselt number based on arithmetic mean temperature difference [3] is usually used. The average Nusselt number thus defined which corresponds to the above two definitions, respectively, becomes

$$\begin{aligned} \overline{Nu}_1 &= -4\int_0^{z}\int_0^{\pi}(\partial\theta/\partial r)_{r=1}\,d\phi\,dz/[\pi z(1+\theta_b)]\\ \overline{Nu}_2 &= -\int_0^{z}\int_0^{\pi}\int_0^{1}(\partial\theta/\partial z)w_f\,r\,dr\,d\phi\,dz/[\pi z(1+\theta_b)]. \end{aligned} \tag{6}$$

3. NUMERICAL SOLUTION

The parabolic-type energy equation is solved by applying the DuFort–Frankel explicit method using the mesh sizes $M \times N = 40 \times 24$. Near the thermal entrance, the variation of the temperature field near the wall with the axial distance is large and a very small axial step Δz is required for accurate solution. With a small Δz the number of axial steps required to reach a fully-developed state may become prohibitively large. Thus, a continually increasing unequal axial step is employed to facilitate the computation. The axial step sizes used vary from 10^{-7} near the entrance to 2×10^{-4} for $z \geqq 10^{-1}$. Some details on the modification for unequal axial step and a starting procedure for the DuFort–Frankel method are given in [10].

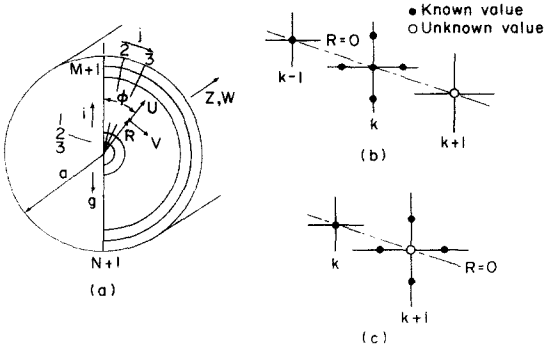

FIG. 1. Coordinate system and treatment of center point.

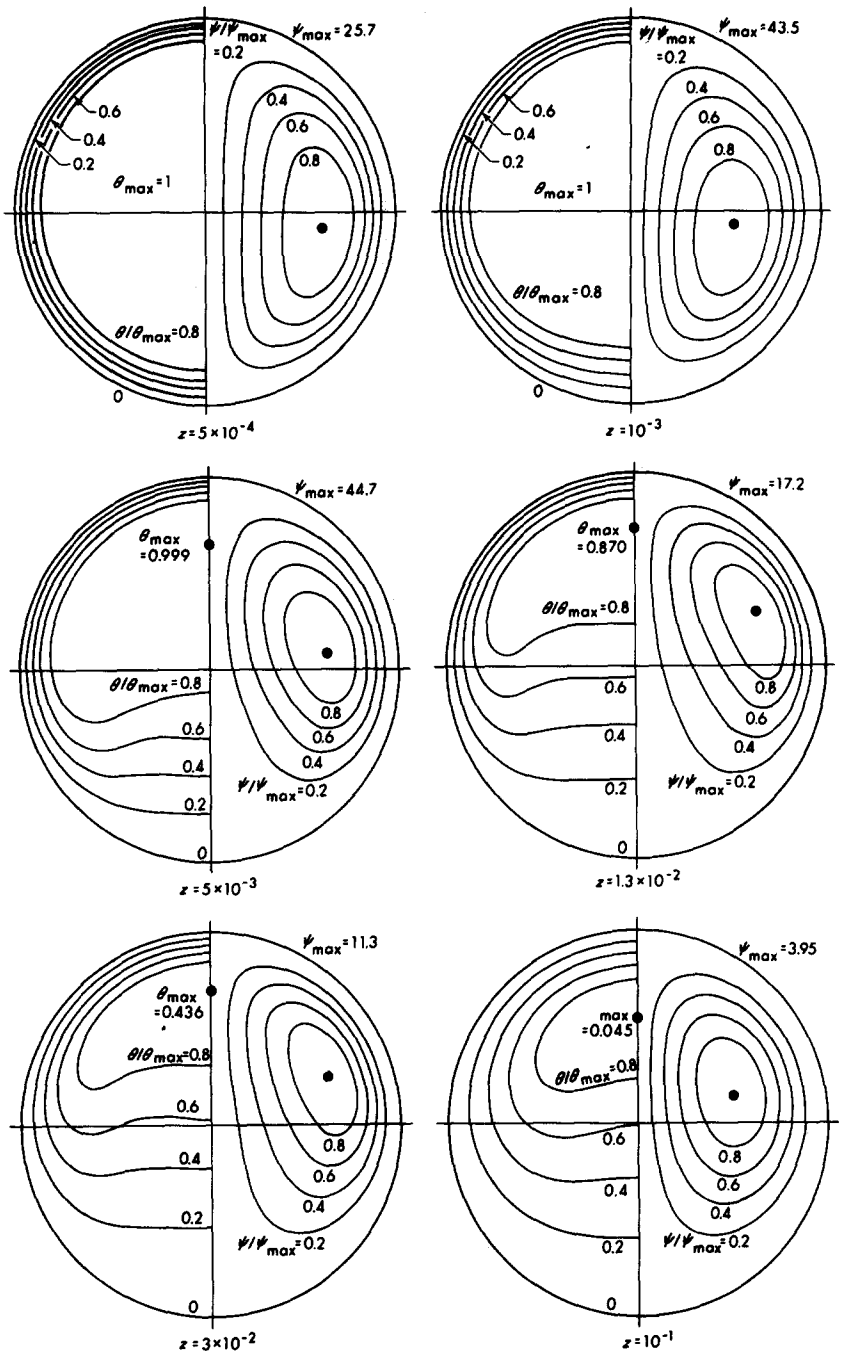

FIG. 2. Development of streamline patterns and isotherms for $Ra = 5 \times 10^4$.

In order to avoid the singularity at the origin of the polar coordinates, a finite-difference equation in Cartesian coordinate is used at the center point. However, a straight-forward application of the DuFort–Frankel method based on central-difference approximation [see Fig. 1(b)] for the axial derivative $\partial\theta/\partial z$ leads to some irregularity in temperature solution near the center point. At a lower Rayleigh number, the irregularity takes the form of temperature depression ($\theta < 1$) at the center point near the thermal entrance where one knows that the temperature profile is still uniform ($\theta = 1$). At a higher Rayleigh number the overshoot ($\theta > 1$) of the center temperature occurs and persists to the downstream region. It is found that the irregularity eventually leads to the unstable and divergent solution. The difficulty can be avoided by using a different calculation procedure as shown in Fig. 1(c). A centerpoint temperature is calculated by using the neighboring four points and a simple forward difference for the axial derivative $\partial\theta/\partial z$.

The vorticity transport equation is solved by using a line iterative method. The calculation proceeds with an initial sweep in the tangential direction followed by a second sweep in the opposite direction. In this study, the calculation is actually terminated after carrying out the two sweeps. To ensure a reasonable computational

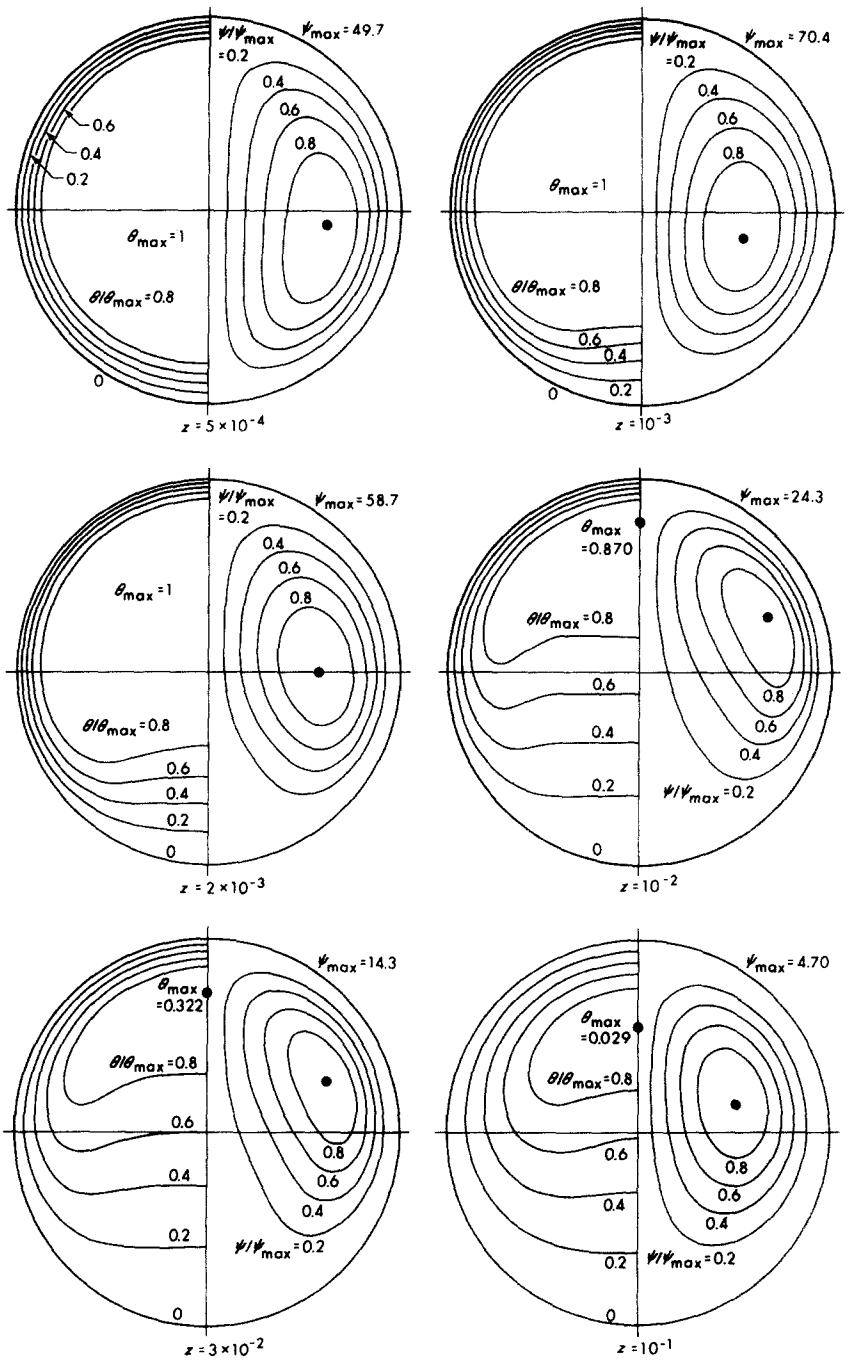

FIG. 3. Development of streamline patterns and isotherms for $Ra = 10^5$.

accuracy with a maximum relative error less than 10^{-3} for the vorticity, the axial step sizes are adjusted by carrying out the numerical experiments.

The elliptic equation (2) for stream function is solved by point SOR, and new boundary vorticity values computed by $\xi_{N+1} = 2\psi_N/(\Delta r)^2$. The iteration for ψ at any axial step using the relaxation factor unity found by numerical experiment is terminated when the error criterion based on the maximum relative error of 5×10^{-4} is satisfied. The required number of iterations is generally less than 10 near the thermal entrance or in the region with considerable natural convection effect and only 2 or 3 for most other axial steps. The values of u and v are found using three-point central difference formula.

The two methods of evaluating the Nusselt number provide a means of assessing the accuracy of the numerical solution. The numerical integration is performed by using Simpson's rule. The deviation of Nu_1 or Nu_2 from the average value ranges from 0.1 to 0.5%. The total number of axial steps and computing time required to reach the asymptotic state depend on Rayleigh number. At $Ra = 5 \times 10^4$, for example, it takes 1688 steps to reach $\theta_b = 0.01$ and the total CPU time is 270 s on AMDAHL 470V/6. At $Ra = 10^5$, the total number of steps is 1490 to reach $\theta_b = 0.015$ and

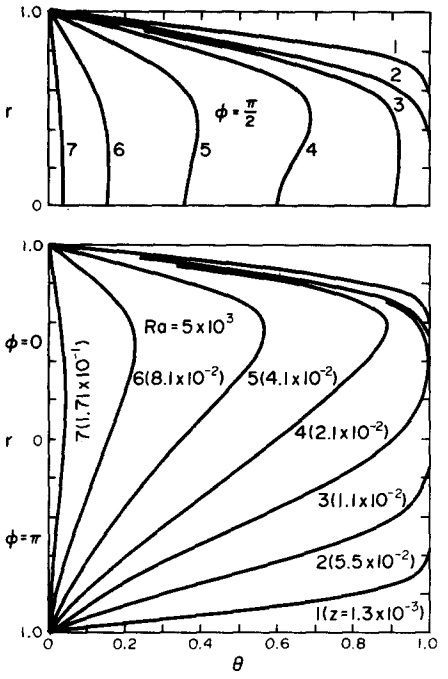

FIG. 4. Developing temperature profiles along horizontal and vertical center lines for $Ra = 5 \times 10^3$.

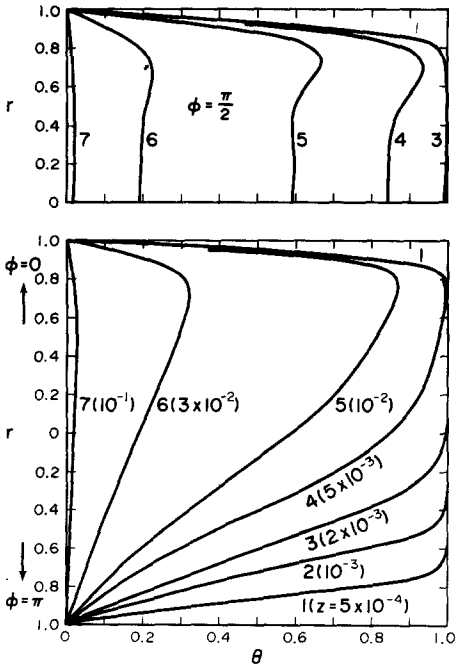

FIG. 5. Developing temperature profiles along horizontal and vertical center lines for $Ra = 10^5$.

the total CPU time is 425 s. With the numerical method used, the computing cost becomes prohibitive for $Ra > 10^6$.

It may be of some interest to point out that the present problem was also solved on IBM 360/67 using the line iterative method for the two elliptic equations and the ADI method of Peaceman–Rachford similar to those employed in [5, 7]. However, it was found that the oscillatory behavior for local Nusselt number appears before reaching the asymptotic value ($Nu_\infty = 3.66$) and the asymptotic solution cannot be obtained for $Ra \geqq 10^4$. Excluding the numerical difficulty noted above, the two numerical solutions agree well for the range of Rayleigh numbers investigated.

4. RESULTS AND DISCUSSION

4.1. *Secondary flow and temperature fields*

Flow visualization is possible by plotting the streamline patterns and isotherms at a series of downstream axial positions and the results are shown in Figs. 2 and 3 for $Ra = 5 \times 10^4$ and 10^5, respectively. In studying the growth and decay of secondary flow field, it is useful to note that the maximum value of the stream function represents the intensity of the secondary motion. The locations of the eyes of the vortices along the axial positions are of special interest. Near the thermal entrance say, $z < 5 \times 10^{-4}$, the isothermals are concentric circles and the gradual distortion of the isotherms near the lower region occurs further downstream. In the lower region, the cooler liquid near the wall is constantly transported downward and the isotherms are sparsely spaced indicating poor wall heat-transfer. On the other hand, near the top of the tube, the warmer liquid in the core region is continually transported upward and the isotherms are closely spaced indicating large local wall heat flux. The development of isothermals along the downstream positions is qualitatively similar to that in the thermal entrance region of curved pipes with uniform wall temperature [11, 12]. In this respect, the development of the isotherms is also somewhat similar to that in transient natural convection in horizontal cylinders with constant cooling rate [10]. The stratification of the flow field in the core region with a vertical temperature gradient at axial position near $z = 10^{-2}$ is of interest.

The developing temperature profiles along $\phi = 0$, π and $\pi/2$ are shown in Figs. 4 and 5 for $Ra = 5 \times 10^3$ and 10^5, respectively, where the curve labelled "7" may be regarded to be a fully developed profile. The secondary velocity profiles for $v(a)$, and $u(b)$ both along the horizontal axis and the distribution of $u(c)$ along the vertical axis are shown in Fig. 6 for the case of $Ra = 10^5$ in order to further study the developing flow fields. In Fig. 6(a) and (c), the increase and subsequent decrease of the secondary velocity component along the axial position can be seen clearly. In Fig. 6(b), the direction of the velocity component u at the far downstream position is seen to be completely opposite to that near the thermal entrance. It is seen that at $z = 10^{-1}$, the secondary flow is quite weak.

The effects of Rayleigh number on the axial distribution of bulk temperature θ_b and local Nusselt number based on the average value of Nu_1 and Nu_2 are shown in Figs. 7 and 8, respectively. For the special limiting case where the fluid is cooled (or heated) nearly to the constant temperature of the tube wall, one obtains the equation of the asymptote $Nu_a = h_a(2a)/k = 1/(2z)$ based on the arithmetic temperature difference $(T_0 - T_w)/2$, [13]. The asymptote Nu_a is also plotted on Fig. 7 and it is clear that without the free convection

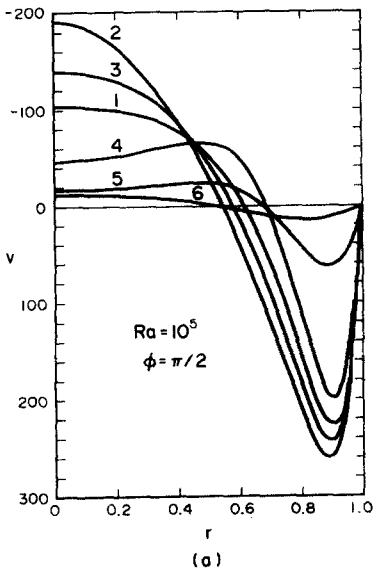

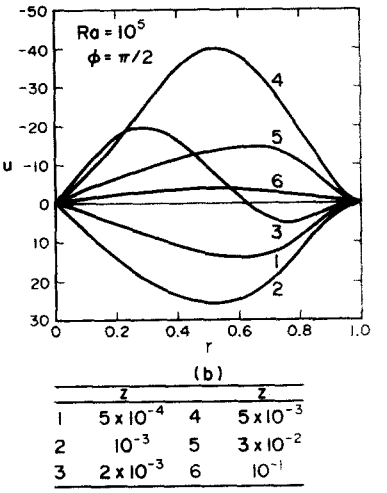

	z		z
1	5×10^{-4}	4	5×10^{-3}
2	10^{-3}	5	3×10^{-2}
3	2×10^{-3}	6	10^{-1}

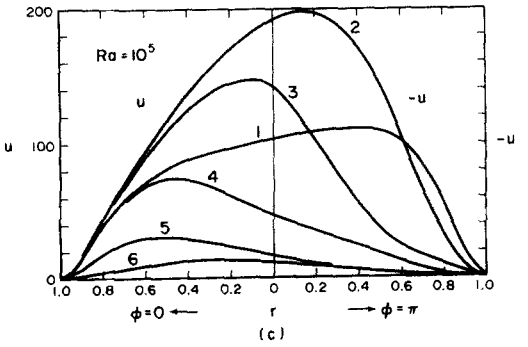

FIG. 6. Development of secondary velocity profiles along horizontal and vertical axes for $Ra = 10^5$.

effect the curve for Nu_a represents an upper bound and the classical Graetz solution $Ra = 0$ is a lower bound. The bulk temperature θ_b at the axial position where the curves for Nu and Nu_a intersect is also marked in Fig. 7 as a solid circle and the numerical value for θ_b is found to be less than 0.08. In practical applications, one may not be concerned with the natural convection effect in the region with $\theta_b < 0.05$ since the effect vanishes as $T_b \to T_w$.

Near the thermal entrance, the natural convection effect is negligible and the Leveque solution applies. One notes that the axial velocity retains a Poiseuille profile in the whole entrance region because of large Prandtl number assumption. Thus, a deviation from the Leveque solution occurs at a certain downstream position depending on Rayleigh number when the convective terms due to secondary flow in energy equation (3) become significant relative to the axial convective term. The numerical results clearly exhibit the existence of a local minimum value for Nu which may signify the balance between the entrance effect due to the axial convective term and the secondary flow effect due to the transverse convective terms. After reaching a local maximum value, the limiting value of $Nu_\infty = 3.66$ is approached asymptotically. At $Ra = 5\times10^5$ and 10^6, the numerical solutions are terminated before reaching the region where Nu decreases monotonically. Because of computing cost, it is impractical to continue the computation further downstream at higher Rayleigh numbers.

Some experimental data from Oliver [14], Depew and Zenter [9], and Depew and August [3] are also plotted in Fig. 8 with the approximate range of Rayleigh and Prandtl numbers indicated for comparison. For

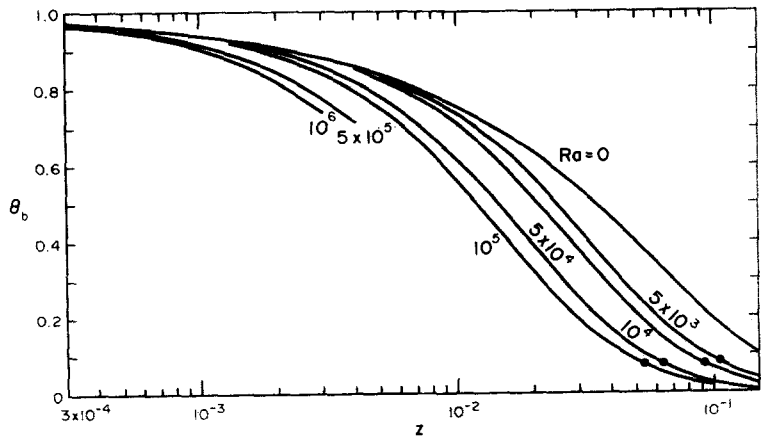

FIG. 7. Rayleigh number effect on axial bulk temperature variation.

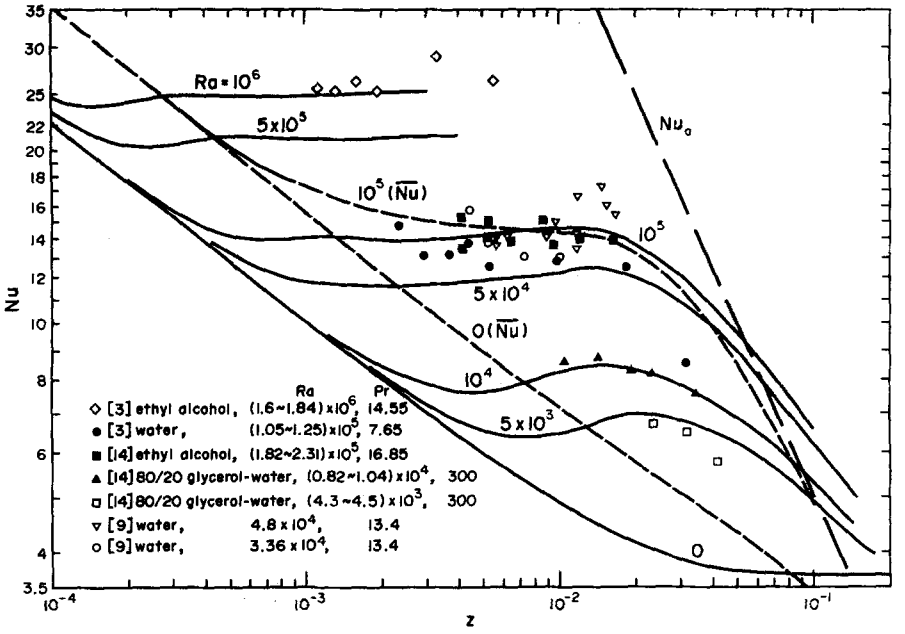

FIG. 8. Local Nusselt number variation with Ra as parameter and comparison with experimental data.

the case $Ra = 10^5$, the average Nusselt number based on the arithmetic mean temperature difference used in experimental investigations [3] is also calculated and the results are shown as a dash-line to facilitate direct comparison with experimental data. Considering the scatter of experimental data, the agreement between theory and experiment for $Ra = 10^5$ can be said to be satisfactory. The calculated average Nusselt number based on arithmetic mean temperature difference from Graetz solution ($Ra = 0$) is also shown in Fig. 8. It is clearly seen that the experimental data are bracketed between the Graetz solution and the asymptote

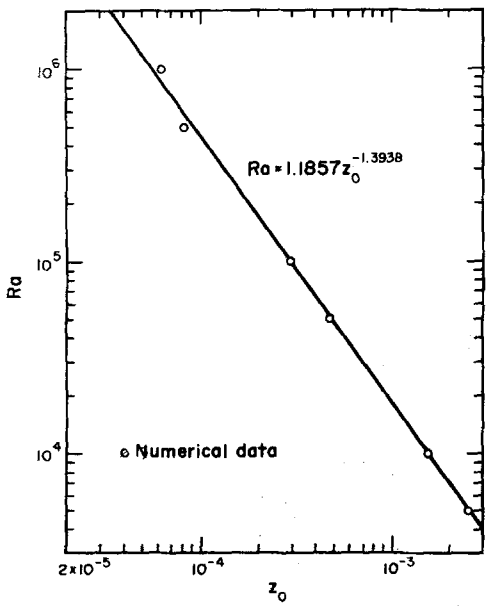

FIG. 9. Correlation for the onset of free convection effect based on 2% deviation of Nu from that of Graetz solution ($Ra = 0$).

$Nu_a = 1/(2z)$ [13]. It is of interest to note that the average Nusselt number based on arithmetic mean temperature difference approaches the asymptote $Nu_a = (1/2z)$ at $z \approx 10^{-1}$. Furthermore, one notes that the average Nusselt number based on $(T_0 - T_w)/2$, [13], and that based on the average mean temperature difference $[(T_0 - T_w) + (T_b - T_w)]/2$, [3], approach to each other as $T_b \to T_w$ at $z \to \infty$.

The deviation of local Nusselt number from Graetz solution is of practical interest and the correlation equation for the prediction on the onset point of free convection effect based on 2% deviation of the local Nusselt number from that of the Graetz solution ($Ra = 0$) is given in Fig. 9 together with the numerical data. From Figs. 8 and 9, it is seen that the free convection effect is significant practically only for the range $z_0 \lesssim z \leqq 2 \times 10^{-1}$. Considering the above observation and the local Nusselt number behavior, one can understand the difficulty in obtaining the correlation equations for heat transfer [3].

5. CONCLUDING REMARKS

The numerical solution is obtained for the Graetz problem with natural convection effect for Rayleigh number up to $Ra = 10^6$. The problem is qualitatively similar to the Graetz problem in curved pipes with constant wall temperature [11, 12]. However, in the latter case the secondary flow is caused by centrifugal forces and an asymptotic value for local Nusselt number exists for a given Dean number. In contrast, for the present problem only one asymptotic value $Nu_\infty = 3.66$ exists for all Rayleigh numbers.

The numerical solution yields detailed streamline patterns and isotherms readily for flow visualization. The free convection effects are known to be significant in a technically important problem of liquid solidification inside a cooled horizontal pipe with forced

laminar flow [8]. Since the boundary conditions are similar, the present numerical results provide some insight and guide in assessing the significance of the free convection effect.

A direct comparison between the present Nusselt number results and those of Hieber and Sreenivasan [4] is not possible since the latter work assumes a uniform axial velocity profile at the thermal entrance and in addition the local Nusselt number is based on $(T_w - T_0)$. Nevertheless, the two results are seen to agree qualitatively and show similar trend.

The present problem is one of the basic convective heat-transfer problems and the assumption of large Prandtl number is practically applicable to Prandtl number greater than order one.

Acknowledgement—This work was supported by the National Research Council of Canada (Grant NRC A1655).

REFERENCES

1. M. Jakob, *Heat Transfer*, Vol. 1, p. 451. John Wiley, New York (1959).
2. E. R. G. Eckert and A. J. Diaguila, Convective heat transfer for mixed, free, and forced flow through tubes, *Trans. Am. Soc. Mech. Engrs* **76**, 497–504 (1954).
3. C. A. Depew and S. E. August, Heat transfer due to combined free and forced convection in a horizontal and isothermal tube, *J. Heat Transfer* **93**, 380–384 (1971).
4. C. A. Hieber and S. K. Sreenivasan, Mixed convection in an isothermally heated horizontal pipe, *Int. J. Heat Mass Transfer* **17**, 1337–1348 (1974).
5. J. W. Ou, K. C. Cheng and R. C. Lin, Natural convection effects on Graetz problem in horizontal rectangular channels with uniform wall temperature for large *Pr*, *Int. J. Heat Mass Transfer* **17**, 835–843 (1974).
6. S. W. Hong, S. M. Morcos and A. E. Bergles, Analytical and experimental results for combined forced and free laminar convection in horizontal tubes, in *Proceedings of the Fifth International Heat Transfer Conference*, NC 4.6, Tokyo (1974).
7. K. C. Cheng and J. W. Ou, Free convection effects on Graetz problem for large Prandtl number fluids in horizontal tubes with uniform wall heat flux, in *Proceedings of the Fifth International Heat Transfer Conference*, NC 4.7, Tokyo (1974).
8. R. D. Zerkle and J. E. Sunderland, The effect of liquid solidification in a tube upon laminar-flow heat transfer and pressure drop, *J. Heat Transfer* **90C**, 183–190 (1968).
9. C. A. Depew and R. C. Zenter, Laminar flow heat transfer and pressure drop with freezing at the wall, *Int. J. Heat Mass Transfer* **12**, 1710–1714 (1969).
10. M. Takeuchi and K. C. Cheng, Transient natural convection in horizontal cylinders with constant cooling rate, *Wärme- und Stoffübertragung* **9**, 215–225 (1976).
11. J. M. Tarbell and M. R. Samuels, Momentum and heat transfer in helical coils, *Chem. Engng Jl* **5**, 117–127 (1973).
12. M. Akiyama and K. C. Cheng, Laminar forced convection in the thermal entrance region of curved pipes with uniform wall temperature, *Can. J. Chem. Engng* **52**, 234–240 (1974).
13. W. H. McAdams, *Heat Transmission*, p. 232. McGraw-Hill, New York (1954).
14. D. R. Oliver, The effect of natural convection on viscous-flow heat transfer in horizontal tubes, *Chem. Engng Sci.* **17**, 335–350 (1962).

EFFETS DE LA CONVECTION NATURELLE SUR LE PROBLEME DE GRAETZ POUR LES TUBES HORIZONTAUX ET ISOTHERMES

Résumé—Le problème classique de Graetz avec effet de convection naturelle, dans des tubes horizontaux chauffés ou refroidis, est approché par une méthode numérique dans une hypothèse large de nombres de Prandtl. Des solutions numériques sont obtenues pour une gamme de nombre de Rayleigh $Ra = 0 \sim 10^6$. Pour étudier l'effet de la convection naturelle, on présente l'écoulement secondaire, le champ de température, la température moyenne, les nombres de Nusselt sont comparés aux données expérimentales et l'accord est trouvé satisfaisant.

DIE AUSWIRKUNG DER FREIEN KONVEKTION AUF DAS GRAETZ-PROBLEM FÜR HORIZONTALE ISOTHERME ROHRE

Zusammenfassung—Das klassische Graetz-Problem in isothermen, gekühlten oder beheizten horizontalen Rohren wird unter Berücksichtigung der freien Konvektion für große Prandtl-Zahlen und für $0 < Ra < 10^6$ numerisch gelöst. Zur Untersuchung des Einflusses der freien Konvektion werden die sich ausbildenden Sekundärströmungen, die Temperaturfelder, die mittlere Temperatur sowie die örtlichen und mittleren Nusselt-Zahlen angegeben. Die errechneten Nusselt-Zahlen werden mit Versuchsergebnissen verglichen, wobei sich befriedigende Übereinstimmung ergibt.

ЭФФЕКТЫ ЕСТЕСТВЕННОЙ КОНВЕКЦИИ В ГОРИЗОНТАЛЬНЫХ ИЗОТЕРМИЧЕСКИХ ТРУБАХ В ЗАДАЧЕ ГРЕТЦА

Аннотация — Численно решается классическая задача Гретца по естественной конвекции в изотермически охлажденных или нагретых горизонтальных трубах в приближении большого числа Прандтля. Численные решения получены для чисел Релея в диапазоне $Ra = 0 \sim 10^6$. При исследовании эффекта естественной конвекции рассматривались развивающееся вторичное течение и температурные поля, средняя массовая тепмература, локальные и средние числа Нуссельта. Расчетные значения числа Нуссельта удовлетворительно согласуются с экспериментальными данными.